

Dynamic Adsorption Behaviors of Various Zeolites for the Adsorbent of Air Separation by Pressure-swing Adsorption Method

By

Yoshitaka OKUGAWA*, Riki SHIBATA* and Tomoyuki INUI*.

(Received October 9, 1987)

Abstract

Adsorption behaviors of O₂ and N₂ in pressure-swing adsorption (PSA) at lower temperature on various American natural zeolites and synthetic zeolites having different pore structures were studied. The adsorption properties were largely dependent on whether the dimension of the pore-structure connection is one or three. Molecular sieves MS-5 A and MS-4 A, which have a large amount of adsorption and a large difference in adsorption capacity for N₂ and O₂, were preferable to air separation by the PSA method. The applicability to the air separation at low temperature was also investigated by using MS-4 A and MS-5 A as the adsorbent. Highly concentrated N₂ was obtained by MS-5 A in the elution period and by MS-4 A in the adsorption period. Furthermore, the applicability to the air separation at room temperature was examined by using MS-4 A as the adsorbent, and the separation was confirmed at this condition.

1. Introduction

Oxygen-rich air is in demand for medical use and chemical oxidation processes. O₂-poor nitrogen gas is needed for freezing food or purging apparatus chambers. For these purposes, not so high purity gas can be sufficiently used. However, ultra high purity N₂ gas has been required for the semiconductor industry, especially for LSI manufacturing. Therefore, a method for effective air separation is strongly required. Cryogenic fractionation has been used conventionally in N₂ and O₂ production from air. Recently, the PSA (Pressure-swing Adsorption) method attracts a great deal of attention because of its energy saving features.^{1~3)} Some small scale plants have been practically operating. Two types of adsorbent, i. e., molecular sieve carbons (MSC)⁴⁾ and zeolites¹⁾, have

* Department of Hydrocarbon Chemistry, Faculty of Engineering, Kyoto University, Sakyo-ku Kyoto 606, Japan

been used in air separation by PSA plants. Although the adsorption amount of O₂ for MSC at the equilibrium condition is similar to that of N₂, the diffusion rate of O₂ in MSC is much faster than that of N₂. Therefore, the difference in this diffusion rate is applied to the separation of O₂ and N₂ in air. The disadvantage of this method is considered to be a short pressure-swing interval and an incomplete separation of O₂ and N₂. On the other hand, since zeolite can take a variety of pore structures, it is possible to separate air into O₂ and N₂ more completely than MSC. However, the relation between the adsorption properties of O₂ and N₂ in the PSA method and the pore structures of zeolites have not been studied extensively.

In this study, the adsorption and desorption properties for O₂ and N₂ on five different kinds of natural zeolites and four kinds of synthetic zeolites were investigated. The correlation between the adsorption characteristics and the physical properties was examined. Successively, the air separations by the PSA method using these zeolites as the adsorbent at low temperatures and room temperature were measured.

2. Experimental

2.1. Zeolite sample

Five kinds of American natural zeolites; chabazite, clinoptilolite, mordenite, ferrierite, and erionite were used. These samples were directly collected from the States of Oregon, Idaho, and Nevada by one of the authors when the Zeotrip '83 was held by the International Committee on Natural Zeolites as the optional tour of 6th International Conference of Zeolite at Reno. The identification of the crystal structures and the chemical composition of these zeolites had been precisely determined by R. A. Sheppard et al⁵⁾. Four kinds of synthetic zeolites: MS-3 A, 4 A, 5 A, and 13 X, manufactured by Union Carbide Co. were used. Each natural zeolite was crushed and ground in a mortar, followed by heating at 350° C for 1 h. This calcined powder was then molded by a tablet machine and crashed into 8 ~ 15 mesh to provide the adsorption experiments.

2.2. Characterization

Morphology of the zeolite crystals was observed by a scanning electron microscope, Hitach-Akashi-102. The X-ray diffraction patterns for each zeolite were measured by CuK α radiation using a Rigaku Denki Gigerflex 2013. The dimension of the pore connection and the mean pore-diameter for each zeolite sample was referred to the literature⁶⁾.

2.3. Method of adsorption measurement

The breakthrough curves for O_2 and N_2 were measured by the dynamic adsorption method. The schematic diagram of the apparatus is shown in Fig. 1. A continuous flow tubular adsorption column equipped with a TCD type gas chromatograph was used. The adsorption measurement was conducted under three different pressures, 2, 6, and 11 kg/cm². The elution was always carried out under atmospheric pressure. The column temperature was controlled at $-75^\circ C$ by dry ice-methanol as the refrigerant. The column length of the adsorbent zeolite was set at 40 mm. The adsorption cylinder was a 316 SUS tube of 6 mm inner diameter. Five percent O_2 or N_2 diluted with He was used as the adsorption gas mixture. The flow rate was settled at 30 ml/min under each operation pressure.

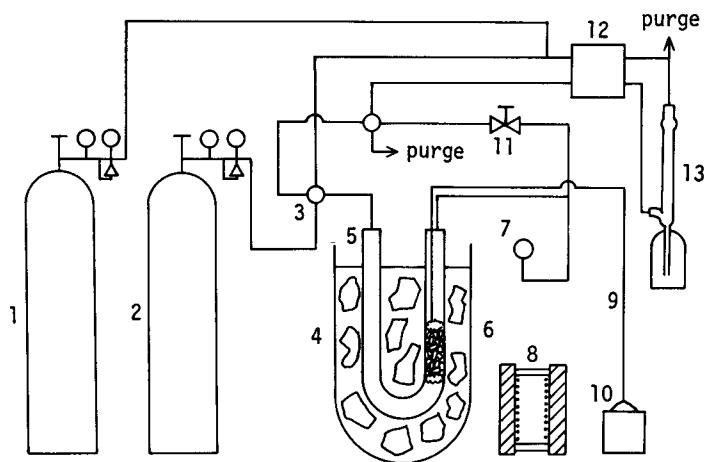


Fig. 1. Schematic diagram of apparatus.

1, GC carrier gas (He) ; 2, adsorption-gas cylinder ; 3, four-way valve ;
 4, refrigerant ; 5, sample column ; 6, adsorbent ; 7, pressure gauge ; 8,
 electric furnace ; 9, thermo-couple ; 10, pyrometer ; 11, flow-control valve ;
 12, TCD cell ; 13, soap film meter.

2.4. Analysis of chromatogram

A typical PSA chromatogram of the O_2 or N_2 adsorption-desorption cycle is illustrated in Fig. 2. The adsorption gas, composed of 5% O_2 or 5% N_2 diluted with He, is introduced under each pressure in a step-function manner at time t_i . During the total adsorption of O_2 or N_2 , no recorder reflection of gas chromatograph is shown. At the time on stream t_b , the breakthrough of O_2 or N_2 occurs. After the recorder reflection reaches the level C_0 , corresponding to the feed concentration, the supply of the adsorption gas is stopped at time t_o . Then,

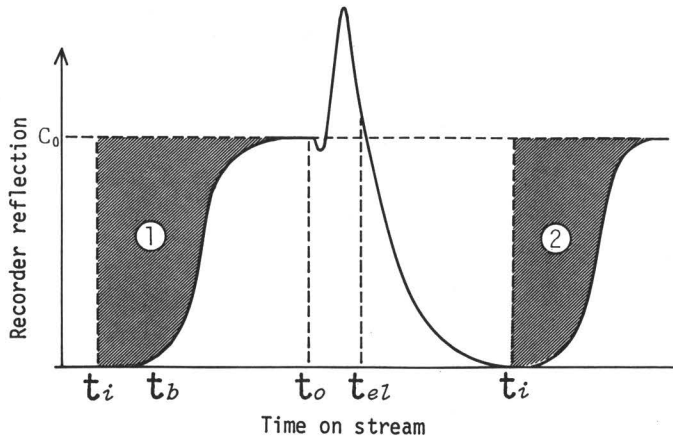


Fig. 2. Illustrative gas chromatograms of the PSA method.

the pressed gas in the adsorption column is reduced to the atmospheric pressure. Helium is then introduced with a flow rate of 30 ml/min at time t_{el} , and the O_2 or N_2 elution is continued. When the recorder reflection drops to the base line, the adsorption gas is introduced again and the same operations are repeated. The Areas 1 and 2 correspond to the amounts of the adsorption at the first and second cycle, respectively. Each area is transformed into the volume of adsorbed O_2 or N_2 per unit weight of the adsorbent. The amount of O_2 or N_2 adsorbed corresponding to Area 1 is defined as the total amount of adsorption, A_T . Area 2 is the apparent reversible adsorption, A_R . In this study, A_T and A_R always show just the same amount indicating that the adsorbed gas is completely desorbed.

2. 5. Air separation by PSA

The air separation experiment was carried out by using a 2. 4 g portion of MS-4 A or MS-5 A. The column temperature was settled at $-75^\circ C$ for each adsorbent, and for MS-5 A also settled at $-18^\circ C$. Before each experiment, the zeolite sample was dried by heating at $350^\circ C$ for 10 min. Air was used as the adsorption gas mixture and the adsorption pressure was settled at 11 kg/cm². The elution was carried out by He under atmospheric pressure. The outlet gas was introduced to the TCD cell, and the breakthrough curves of N_2 and O_2 were recorded. Then, from the outlet of the TCD cell, one ml of the gas mixture was sampled and analyzed by another TCD at every one minute. For air separation at room temperature a larger amount of MS-4 A (6. 7 g) was used as the adsorbent.

3. Results and Discussion

3.1. Morphology of the samples.

The shape and size of the crystalites in the samples were markedly different from each other. Chabazite (sample 1) was highly crystallized having cubic crystals of $4 \sim 7 \mu\text{m}$ in size. Clinoptilolite (sample 2) was an agglomerate of fine ($0.4 \mu\text{m}$) spherical particles. Mordenite (sample 3) showed a fine-pole shape ($0.5 \mu\text{m} \phi \times 5 \mu\text{m}$ length). Ferrierite (sample 4) was also a fine-pole shape but more fine and longer ($0.4 \mu\text{m} \phi \times \text{ca. } 14 \mu\text{m}$ length) than sample 3. Erionite (sample 5) had a fine fibrous shape ($0.2 \mu\text{m} \phi \times 18 \mu\text{m}$). All synthetic zeolites (samples 6 through 9) were highly crystallized uniform particles of about $2 \mu\text{m}$. Pore sizes of the major zeolite components in the natural zeolite samples and the dimensions of their pore connections are shown in Table 1. The crystal structures of the zeolite samples were determined by XRD-patterns and were referring to the description in the literature⁵⁾.

3.2. Adsorption properties of zeolite samples

Adsorption properties of zeolite samples for O_2 and N_2 under different adsorption pressures are shown in Figs. 3 and 4. In every zeolite sample, the adsorption amounts for O_2 and N_2 were proportional to the adsorption pressure. This linearity may be explained as follows. The maximum N_2 adsorption

Table 1 Physical properties and adsorption characteristics for each zeolite.

Sample No	Zeolite	pore diameter (A)	dimension of pore-connection	O_2		N_2	
				a	b	a	b
1	Chabazite	3.6×3.7	3	2.6	15.8	2.1	28.4
2	Clinoptilolite	4.0×4.5 4.4×9.2	1	1.0	11.7	0.4	6.3
3	Mordenite	2.9×5.7 6.7×7.0	1	1.5	11.1	1.3	17.7
4	Ferrierite	3.4×4.8 4.3×5.5	1	1.7	9.6	1.0	23.6
5	Erionite	3.6×5.2	3	1.6	9.5	1.1	18.1
6	MS-3A	3	3	0	6.5	0	7.2
7	MS-4A	3.5	3	3.1	4.4	0	5.6
8	MS-5A	4.2	3	3.5	6.0	3.3	43.1
9	MS-13X	10	3	2.1	5.2	3.6	20.9

a: gradient, b: amount at 1 kg/cm^2

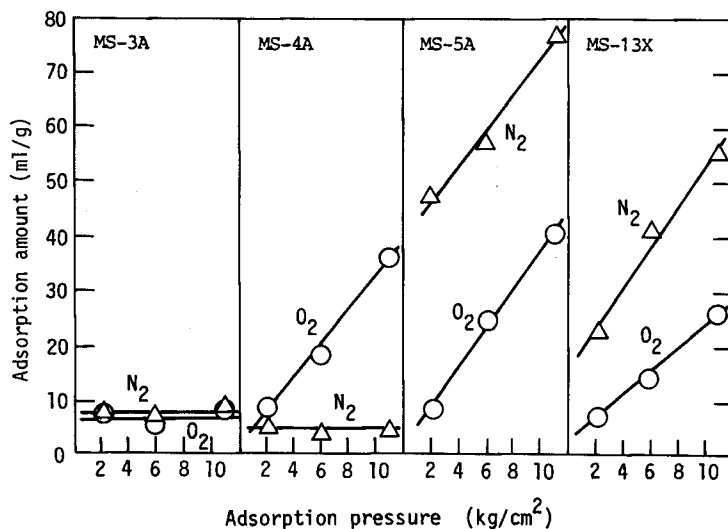


Fig. 3. Pressure dependence of the amount of adsorbed O₂ and N₂ for various synthetic zeolites.

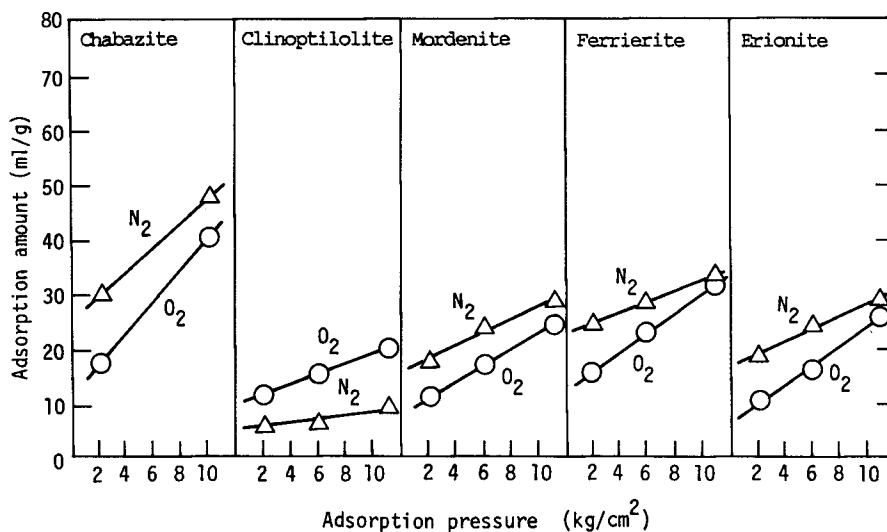


Fig. 4. Pressure dependence of the amount of adsorbed O₂ and N₂ for various natural zeolites.

amount among all samples was observed in MS-5 A. MS-5 A has a pore volume 0.27 ml/g. About 80 ml/g N₂ gas was adsorbed at 11 kg/cm². This amount corresponds to 0.05 ml N₂ liquid per gram. Therefore, only 1/5 of the pore volume is occupied by N₂ molecules in this case. The adsorption amount must increase with an increase of the adsorption pressure in such a low occupancy region. We

can expect the proportionality as observed. These linear relationships were expressed by using gradient **a** and the intercept **b** at the adsorption pressure 1 kg/cm², under which desorption is operated. The values **a** and **b** are summarized in Table 1. The gradients **a**'s for both N₂ and O₂ on MS-3 A and for N₂ on MS-4 A became zero. This indicated the molecular-sieving effects due to their relatively narrow pore diameter, compared with the molecular kinetic diameter of O₂ and N₂. The value **b** would be regarded as an indication to evaluate the adsorption ability for each zeolite. Values **b** for N₂ are larger than those for O₂, except clinoptilolite. As is well known, N₂ molecule has a slightly larger quadrupole moment than the O₂ molecule. Therefore, N₂ is more strongly adsorbed on the active site of zeolite than O₂. The gradients **a**'s are classified into two groups. The smaller value group and the larger one correspond to the dimension of pore connection one or three, respectively. In Fig. 3, the effects of the pore diameters are clearly shown in the gradients for O₂ and N₂. For MS-5 A and MS-13 X, the pore diameters are large enough for O₂ and N₂ to pass through. On the other hand, for MS-3 A, both O₂ and N₂ cannot pass through the pore. For MS-4 A, which has a medium pore size, only oxygen can pass through the pore. In Fig. 4, the pressure dependence of adsorption amounts of O₂ and N₂ for the natural zeolites are shown. Except for chabazite, these natural zeolites adsorb O₂ and N₂ with a similar pressure dependence, and the amounts of adsorption are small. Only chabazite has a larger adsorption capacity, the same as MS-13 X. Although both chabazite and erionite have the three dimensional pore connection, and the pore diameter of erionite is rather larger than that of chabazite, the adsorption amount of erionite is smaller than that of chabazite. The reason for this apparent discrepancy may be explained as follows. As shown in Fig. 5, for chabazite, adsorption molecules can straightly transport from one 8-membered ring opening (one of the shadowed parts) to another. In contrast with this, for erionite the molecule which entered from one pore must turn its direction to get out. Consequently, despite its three dimensional pore structure, the mass transfer resistance in erionite must be larger than that in chabazite. The adsorption properties resemble the one dimensional ones, whose mass transfer resistance is much larger than that of the three dimensional one. As the adsorbent for air separation, a large adsorption amount and a large difference in adsorption capacity for N₂ and O₂ are needed. Therefore, zeolites which have a one dimensional pore connection are unsuitable for air separation. Further, chabazite, which shows a nearly equal amount of N₂ and O₂ adsorption is also unsuitable. Since MS-5 A largely adsorbs both N₂ and O₂, air separation must be difficult. However, the adsorption amount of N₂ is so large that after

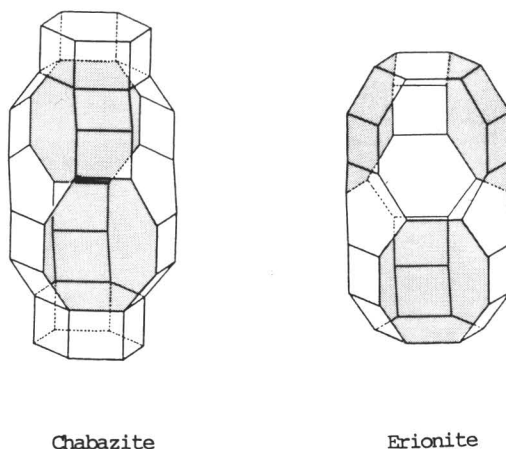


Fig. 5. Crystalline structure of Chabazite and Erionite. Shaded parts show pore opening areas.

the O_2 elution, N_2 still continues its elution. Therefore N_2 separation can be expected.

3. 3. Air separation by PSA method

The air separation experiments with MS-5 A at -75 and $-18^\circ C$ are shown in Figs. 6 and 7, respectively. In each figure, changes in concentration of the elution gases are shown. Before t_{el} , the composition of elution gas is nearly the same as the air, because the air in the dead space of the column flowed out by expanding the volume with a reduction of the pressure. After this period, desorption of the adsorbed gas molecules begins. The calculated N_2 fraction in this desorption period is also shown in the same figure. After finishing the O_2 elution, pure N_2 is obtained. The slow elution of N_2 is due to its large amount of adsorption and its stronger adsorption force. In Fig. 6, the N_2 gas corresponding to the shaded part is calculated as 22.9 litres with 97% purity per one litre MS-5 A. As shown in Figure 7, 14.9 litres of 96% purity N_2 is obtained for one litre MS-5 A at $-18^\circ C$. The amount of N_2 obtained at $-18^\circ C$ is smaller than that at $-75^\circ C$. However, since the period of collecting the effluent gas at $-18^\circ C$ is shorter, the PSA cycle time can be shortened. It takes much time to regenerate the adsorption bed at $-75^\circ C$, because of a stronger adsorption force and a larger amount of adsorption of N_2 . This is a serious disadvantage for the separation process by MS-5 A from the viewpoint of efficiency.

As can be understood from Fig. 3, MS-4 A adsorbed O_2 in proportion to the adsorption pressure, whereas N_2 adsorbed very little irrespective of the pressure.

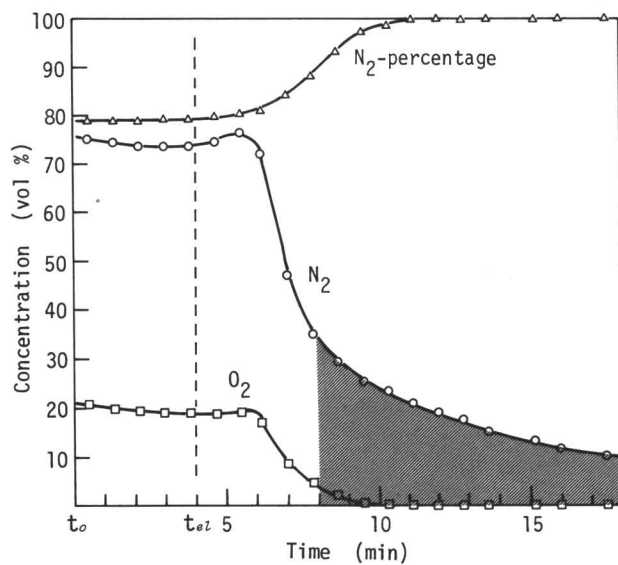


Fig. 6. Elution curves in air adsorption for MS-5 A at -75°C .

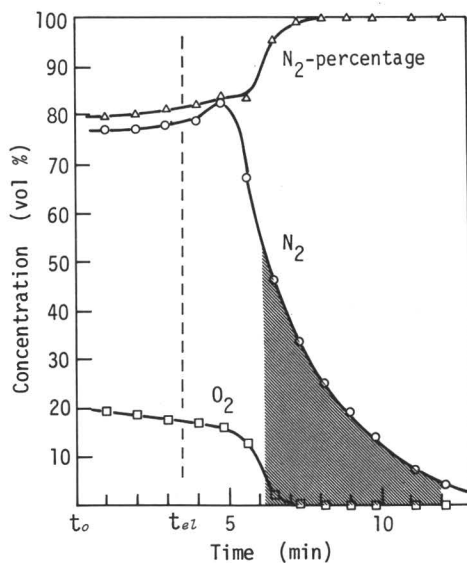


Fig. 7. Elution curves in air adsorption for MS-5 A at -18°C .

Therefore, it is expected that high purity N_2 or O_2 is obtained by the PSA method. Fig. 8 shows the concentration change of N_2 and O_2 in the effluent gas of the air separation experiment by using MS-4 A at -75°C . The balance is the carrier gas Helium. The broken line in this figure shows the change in N_2

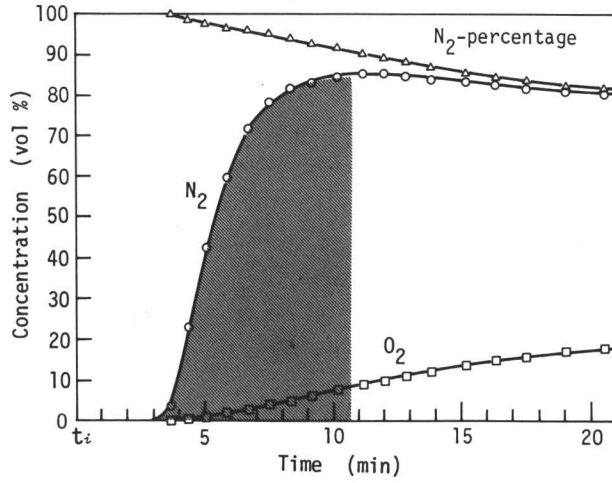


Fig. 8. Breakthrough curves in air adsorption for MS-4 A at -75°C .

percentage in the summation of N_2 and O_2 in the effluent gas. The N_2 concentration in the effluent gas rapidly increases after its breakthrough, while the O_2 concentration increased gradually in the same period. Accordingly, the N_2 percentage becomes high. When the effluent gas is gathered until the N_2 percentage drops down to 90%, the average N_2 percentage becomes 95%, and the amount of this gas is 38.8 l/l-MS-4 A. Fig. 9 shows the concentration changes of N_2 and O_2 during the elution processes. After the pressure was reduced to the atmospheric pressure, He was introduced as the carrier gas.

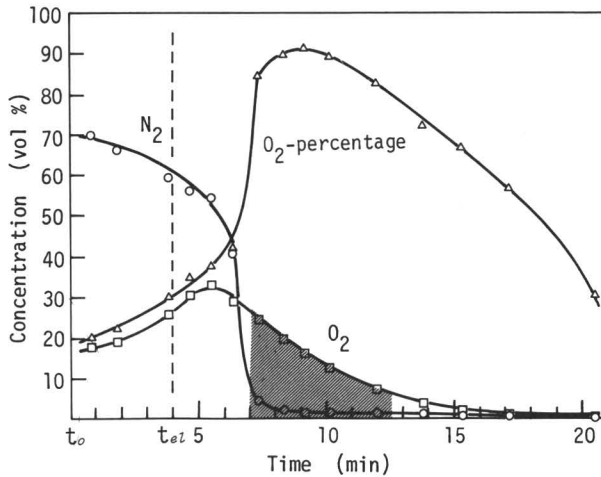


Fig. 9. Elution curves in air adsorption for MS-4 A at -75°C .

Although the N_2 concentration rapidly decreased, the O_2 concentration decreased slowly. Accordingly, the highly concentrated O_2 could be obtained. The shadowed area of Fig. 9 corresponded to 88% O_2 percentage and 4.8 l/l -MS-4 A. The results of the air separation experiments are summarized in Table 2.

Air separation capability of MS-4 A at room temperature was also tested. A 6.7 g portion of MS-4 A was packed in the column. Adsorption pressure was settled at 6 kg/cm^2 . Nitrogen was used as the carrier gas. Therefore, only the change of O_2 concentration was detected by the TCD cell. The results of the measurements are shown in Fig. 10. The periods of adsorption and desorption stages were set at 3 and 8 min, respectively. The adsorption-desorption cycles were repeated 8 times. Except for the first cycle, the same responses were observed repeatedly. The average concentration and amount of N_2 , which was purged during the adsorption stage, was calculated as 93% and 9.3 l/l -MS-4

Table 2 Performance of air separation for MS-5 A and MS-4 A.

Adsorbent	adsorption stage (liter/liter-adsorbent)			desorption stage (liter/liter-adsorbent)		
MS-5 A	cannot be separated			97%	N_2	22.9
MS-4 A	95%	N_2	38.8	88%	O_2	4.8

Operation temperature, $-75^\circ C$. Adsorption pressure, 10 kg/cm^2 .
Desorption pressure, 1 kg/cm^2

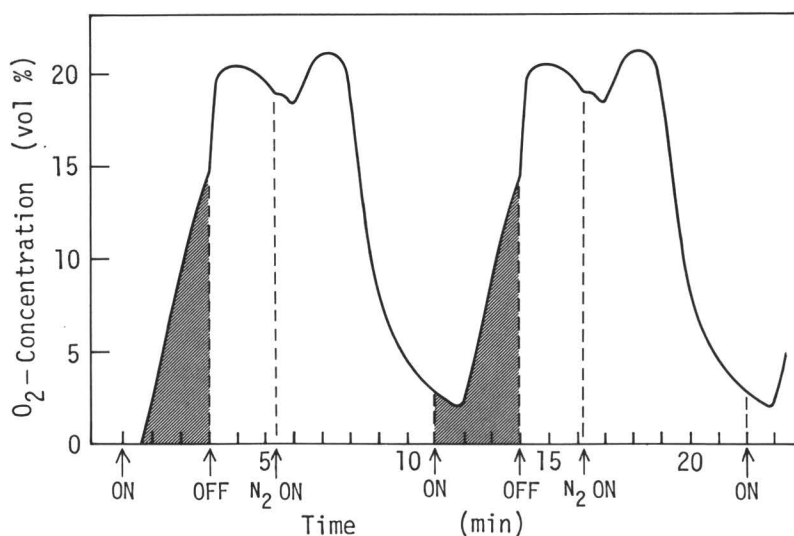


Fig. 10. Breakthrough curves for MS-4 A at room temperature.

A, respectively. This amount of N_2 was about $1/4$ of that obtained by the experiment at $-75^\circ C$.

References

- 1) G. A. Sorial, W. H. Granville, and W. O. Daly, Chem. Engng Sci., **38**, 1517 (1983)
- 2) H. Lee and D. E. Stahl, A. I. Ch. E. Symp. Ser., **69**, 134, 1 (1973)
- 3) J. C. Davis, Chem. Eng., Oct. 16, 88 (1972)
- 4) K. Knoblauch, Chem. Eng., Nov. 6, 87 (1978)
- 5) R. A. Sheppard, A. J. Gude, 3rd, and F. A. Mumpton, Zeo-Trip '83, INTERNATIONAL COMMITTEE ON NATURAL ZEOLITES (1983)
- 6) J. V. Smith, in "Zeolite Chemistry and Catalysis" J. A. Rabo ed., ACS Monograph 171 (1976)
- 7) D. W. Breck, and R. W. Grosa, Preprint 3rd Conf. MS Zeolite, p. 319 (1973)